Eur Biophys J (2000) 29: 146–152

BIOPHYSICS LETTER

C. Keppler · K. Achterhold · A. Ostermann
U. van Bürck · A.I. Chumakov · R. Rüffer
W. Sturhahn · E.E. Alp · F.G. Parak

Nuclear forward scattering of synchrotron radiation by deoxymyoglobin

Received: 30 August 1999 / Revised version: 22 October 1999 / Accepted: 6 December 1999

Abstract Nuclear forward scattering of synchrotron radiation is used to determine the quadrupole splitting and the mean square displacement of the iron atom in deoxymyoglobin in the temperature range between 50 K and 243 K. Above 200 K an abnormally fast decay of the forward scattered intensity at short times after the synchrotron flash is observed, which is caused by protein-specific motions. The results strongly support the picture that protein dynamics seen at the position of the iron can be understood by harmonic motions in the low temperature regime while in the physiological regime diffusive motions in limited space are present. The shape of the resonance broadening function is investigated. An inhomogeneous broadening with a Lorentzian distribution indicating dipole interactions results in a better agreement with the experimental data than the common Gaussian distribution.

Key words Myoglobin · Protein dynamics · Nuclear forward scattering · Mössbauer effect · Synchrotron radiation

Introduction

For many years, Mössbauer spectroscopy using ^{57}Fe has become a powerful tool in biophysics. In general, this technique is used to study the electronic structure of the iron in a compound. In proteins, valuable information on the dynamic properties have been obtained. Using this technique a large number of iron containing proteins have been investigated (for reviews see: Parak and Reinisch 1986; Debrunner 1993; Parak and Frauenfelder 1993). All these measurements have been performed using the conventional Mössbauer absorption technique. A radioactive ^{57}Co source decays and populates the Mössbauer energy level in ^{57}Fe, which emits γ-rays of 14.413 keV energy within a bandwidth of 4.7 neV. The energy of the γ-rays can be tuned by several bandwidths around the resonance energy using the Doppler effect by moving the radioactive source. Under proper conditions the γ-rays can be resonantly reabsorbed by the ^{57}Fe atoms in the sample under investigation. The transmitted intensity as a function of the Doppler velocity is referred to as the conventional Mössbauer absorption spectrum in the following. The electric and magnetic hyperfine fields at the position of the iron nucleus are obtained from the positions of the absorption maxima in the spectrum. They give information on the surroundings of the iron which are influenced by the protein conformation. Dynamics can be investigated by analysing the shape and the area of the absorption spectrum. It has been shown that the mean square displacement, $\langle x^2 \rangle$, of the iron in myoglobin behaves solid-like at temperatures below 180 K (Parak et al. 1982) and can be described by a normal mode analysis (Melchers et al. 1996). At higher temperatures, new types of motions occur, which cause additional broad lines in the Mössbauer absorption spectrum and a strong decrease of the Lamb-Mössbauer factor. These protein-specific motions were interpreted within the Brownian oscillator model as diffusion in a restricted space (Knapp et al. 1983).

Synchrotron radiation offers a number of possibilities to investigate protein dynamics. Phonon spectra of myoglobin have been investigated by the phonon-assisted Mössbauer effect (Achterhold et al. 1996; Keppler et al. 1997). In 1991, another kind of Mössbauer spectroscopy was successfully demonstrated (Hastings et al.

C. Keppler · K. Achterhold · A. Ostermann · F.G. Parak (✉)
Fakultät für Physik E17, Technische Universität München, 85747 Garching, Germany

U. van Bürck
Fakultät für Physik E15, Technische Universität München, 85747 Garching, Germany

A.I. Chumakov · R. Rüffer
European Synchrotron Radiation Facility, BP 220, 38043 Grenoble Cedex, France

W. Sturhahn · E.E. Alp
Advanced Photon Source, Argonne National Laboratory, Argonne, IL 60439, USA

1991): nuclear forward scattering of synchrotron radiation. The very intense, pulsed radiation emitted by a synchrotron is used to excite the Mössbauer level in ^{57}Fe. Since the lifetime of this energy level is rather large ($\tau = 141$ ns), the radiation is reemitted with sufficient delay to be discriminated from the promptly transmitted intensity by suitable time-gated detector systems. Owing to constructive interference the delayed radiation is predominantly scattered in the forward direction. The time dependence of this forward scattered radiation is determined by the hyperfine fields at the iron position and the dynamics of the iron (for a review see Smirnov 1996). Therefore, these time spectra obtain in principle the same information as conventional Mössbauer absorption spectra. However, the sensitivity of both techniques differ. For example, while broad lines, reflecting the protein-specific dynamics, reveal themselves in the region of large velocities in the Mössbauer absorption technique, they occur at short times in the time domain Mössbauer spectroscopy. In the absorption experiments, the broad lines are not separable from the merely transmitted radiation. In the time domain experiment, the counting rates at short times are large and the fast drop-off due to broad lines is clearly separable from the ordinary later time course. The development of third-generation synchrotrons has made it now possible to perform nuclear forward scattering on samples with very low ^{57}Fe content, such as proteins. This work presents measurements on deoxymyoglobin obtained with this new technique.

Materials and methods

The heme group of sperm whale myoglobin (Sigma) was extracted with 2-butanone at pH 2.3 and substituted by hemin enriched in ^{57}Fe according to Teale (1959). The resulting metmyoglobin solution was purified with a cation exchange chromatography column (SP-sepharose) on Pharmacia FPLC equipment. Metmyoglobin crystals were grown in the space group $P2_1$ with the batch method at pH 6.8 from a solution containing 3.2 M $(NH_4)_2SO_4$ and 50 mM Na_3PO_4. The myoglobin concentration in the crystallisation batches was 30 mg/ml. The crystals were collected and washed with a solution containing 3.4 M $(NH_4)_2SO_4$ and 50 mM Na_3PO_4 adjusted to pH 6.8. The crystals were deoxygenated and reduced by a stepwise addition of sodium dithionite until a 20-fold excess was reached. The deoxymyoglobin crystals were cleaned from superfluous buffer on the surface and filled in a plastic sample holder. The reduction and the filling of the sample holder was performed under an argon atmosphere. Immediately after the sample preparation a conventional Mössbauer spectrum was taken to control the complete reduction of the sample.

The experiments were performed at the undulator beamlines 3ID at the Advanced Photon Source (APS) (Alp et al. 1994) and BL11/ID18 at the European Synchrotron Radiation Facility (ESRF) (Rüffer and Chumakov 1996). In these facilities, ultrarelativistic electrons are kept in a storage ring in a closed orbit. The time width of each synchrotron pulse is less than 0.1 ns. The measurements were performed in the "6 + 22 singlets" mode of the APS and "16-bunch" mode of the ESRF. The distance between two bunches is 176 ns in the "16-bunch" mode. The spacing between the 22 singlets, which were exclusively used in the experiment at the APS, is 147.7 ns. The electrons produce intense X-rays due to acceleration while traversing an undulator optimised to emit radiation of 14.413 keV energy of some hundred eV bandwidth. This radiation, which has the same time structure as the electrons in the storage ring, is monochromised to a very small bandwidth in the order of meV magnitude around the Mössbauer energy to reduce radiation damage in the sample and overloading of the detector system. The X-ray pulses pass the sample, which is placed in a liquid helium cryostat. The promptly transmitted intensity and the delayed forward-scattered radiation are detected by an avalanche photodiode (APD) (Baron 1995), which is placed downstream in the forward direction. The time resolution of the APD is better than 1 ns; the efficiency for the 14.4 keV radiation is about 25% for a perpendicular incidence. A fast timing electronics based on a time to amplitude converter (TAC), an analog to digital converter (ADC) and a PC-based multichannel analyser (MCA) is used to acquire the data. A reference timing signal from the synchrotron bunch clock synchronises the electronics with the electron bunches of the ring. In order not to overwhelm the signal processing electronics, the prompt signal is gated by a logic coincidence unit.

For the measurements at the APS the energy width of the beam was 0.85 meV (Toellner et al. 1997). The intensity of the forward scattered radiation was recorded in the time window between 25 ns and 118 ns after the prompt X-ray flash. Nuclear forward spectra of deoxymyoglobin crystals were taken at 14 different temperatures in the temperature range between 50 K and 243 K. Some of the spectra are shown in Fig. 1. The measuring time for each spectrum was increased with increasing temperature owing to a decreasing Lamb-Mössbauer factor. While the spectrum at 50 K was taken within 15 min, the measuring time for the spectrum at 243 K was 3 h. The whole dataset was obtained within 30 h.

For the experiments at the ESRF, another sample of deoxymyoglobin crystals was used. Here, the energy width of the incoming beam was 4.4 meV. The delayed intensity was recorded in the time window between 10 ns and 152 ns. The measuring time for each spectrum was approximately 65 min. The spectra are shown in Fig. 2.

Results

The synchrotron pulse with an energy width in the meV region excites all allowed ^{57}Fe Mössbauer transition

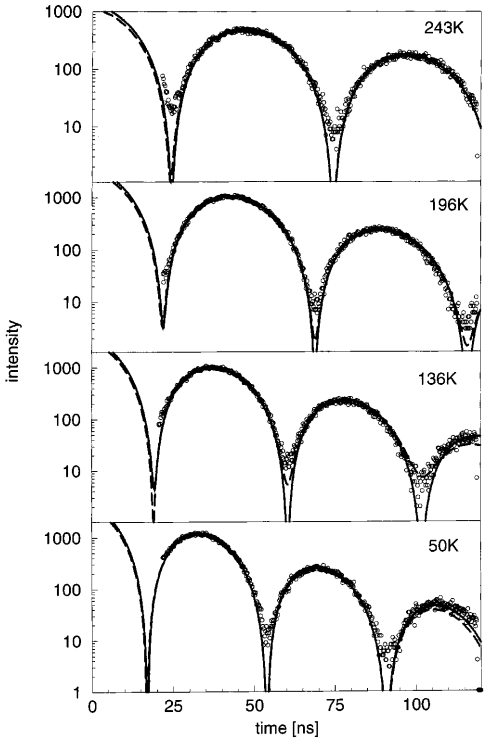

Fig. 1 Nuclear forward scattering spectra of deoxymyoglobin crystals at selected temperatures measured at the APS. *Solid line*: least squares fits using Eqs. (1), (2), (7) and (9) and a distribution function of Lorentzian shape of width $\Delta = 1.2\Gamma_{\mathrm{nat}}$. *Dashed line*: least squares fits using Eqs. (1), (2), (7) and (9) and a Gaussian distribution function for inhomogeneous broadening of width $\Delta = 1.2\Gamma_{\mathrm{nat}}$

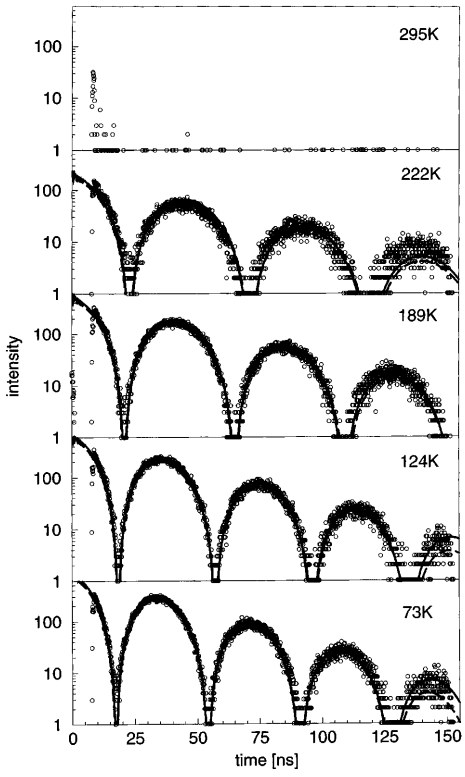

Fig. 2 Nuclear forward scattering spectra of deoxymyoglobin crystals measured at the ESRF. The data acquisition took approximately 65 min for each spectrum. *Solid line*: least squares fits using Eqs. (1), (2), (7) and (9) and a distribution function of Lorentzian shape of width $\Delta = 1.2\Gamma_{\mathrm{nat}}$. *Dashed line*: least squares fits using Eqs. (1), (2), (7) and (9) and a Gaussian distribution function for inhomogeneous broadening of width $\Delta = 1.2\Gamma_{\mathrm{nat}}$. The data acquisition at 295 K shows that the background radiation and detector noise contributes less than 7 counts per channel at times larger 10 ns

energies in the sample coherently, so that their interference has to be taken into account for data evaluation. We characterise the amplitude of the electromagnetic wave by its magnetic component B. The transmitted wave is then B_{tr}. Measuring the nuclear forward scattering as a function of time t, one obtains the intensity:

$$I(t) = B_{\mathrm{tr}}(t)B^{*}_{\mathrm{tr}}(t) \tag{1}$$

where

$$B_{\mathrm{tr}}(t) = \int B_{\mathrm{tr}}(\omega)\exp(i\omega t)\mathrm{d}\omega \tag{2}$$

We have now to calculate $B_{\mathrm{tr}}(\omega)$. For the further analysis of the measured spectra a rather simple approach is chosen (van Bürck et al. 1992), where the sample is characterised by a nuclear refractive index $n(\omega)$. This can easily be visualised. The incident beam travels through the sample and interferes with the waves scattered by the ^{57}Fe nuclei. Using the Fresnel zone construction, one sees that one half of the spherical waves of the first Fresnel zone contribute to the forward scattering from each slice of the sample. The change of the transmitted wave in a slice of the sample becomes

$$\mathrm{d}B_{\mathrm{tr}} = B_{\mathrm{tr}} i\lambda f_{\mathrm{N}} \mathrm{d}n_{\mathrm{N}} \tag{3}$$

where f_{N} is the nuclear forward scattering amplitude of ^{57}Fe, n_{N} the number of ^{57}Fe/cm^2 and λ the wavelength of the ^{57}Fe radiation. For one single isolated resonance f_{N} becomes

$$f_{\mathrm{N}} = -\frac{\mathrm{k}}{4\pi}\sigma_0 f \frac{\frac{\Gamma_{\mathrm{nat}}}{2}}{\hbar(\omega-\omega_0) + i\frac{\Gamma_{\mathrm{nat}}}{2}} \tag{4}$$

Here $\hbar\omega_0$ is the resonance energy of the Mössbauer transition, $\sigma_0 = 2.56 \times 10^{-18}$ cm^2 its resonant cross section and $\Gamma_{\mathrm{nat}} = 4.7 \times 10^{-9}$ eV its natural halfwidth; k is the wavevector of the radiation and f the Lamb-Mössbauer factor of the sample. After crossing the investigated material with the geometrical thickness d the transmitted wave becomes

$$B_{\mathrm{tr}} = B_0 \exp\left[ik\left(1 + \frac{\lambda f_{\mathrm{N}} n_{\mathrm{N}}}{kd}\right)d\right] \tag{5}$$

where $B_0\exp(ikd)$ is the incoming wave transmitted without interaction. Note that the phase factor depending on the sample thickness d disappears when an intensity is measured. Comparing the k-vector within the medium, k_{Med}, and the vacuum wavevector k one obtains the nuclear refraction index $n(\omega)$:

$$n(\omega) = \frac{k_{\mathrm{Med}}}{k} = 1 + \frac{\lambda f_{\mathrm{N}} n_{\mathrm{N}}}{kd} \tag{6}$$

The amplitude of the wave transmitted by the medium can now be written:

$$B_{\mathrm{tr}}(\omega) = B_0 \exp(in(\omega)kd) \tag{7}$$

From Eqs. (4) and (6) the refractive index $n(\omega)$ for one single isolated resonance becomes

$$n(\omega) = 1 - \frac{T_{\mathrm{eff}}}{2kd} \frac{\frac{\Gamma_{\mathrm{nat}}}{2}}{\hbar(\omega - \omega_0) + i\frac{\Gamma_{\mathrm{nat}}}{2}} \tag{8}$$

where the effective thickness T_{eff} is defined by $T_{\mathrm{eff}} = n_{\mathrm{N}} f \sigma_0$. In deoxymyoglobin the electric quadrupole interaction yields two resonances separated by the quadrupole splitting $\hbar\Delta\omega_{\mathrm{Q}}$. Furthermore, one has to take into consideration that each protein molecule may be frozen in a slightly different conformational substate (Frauenfelder et al. 1988). Therefore, the iron atom of each molecule is situated in a slightly different environment and the resonance energies are a little shifted. This effect yields a temperature-independent inhomogeneous line broadening in conventional Mössbauer absorption spectroscopy. The inhomogeneous broadening is treated according to Smirnov (1996) and Shvyd'ko et al. (1998). The refractive index $n(\omega)$ is convoluted with a broadening function $F(\omega)$ of Lorentzian or Gaussian shape with full width, Δ, at half maximum (FWHM). Taking into account the quadrupole splitting and inhomogeneous broadening, the refractive index for deoxymyoglobin can be written in the following way:

$$n(\omega) = F(\omega) \otimes \left[1 - \frac{T_{\mathrm{eff}}}{4kd}\left(\frac{\frac{\Gamma_{\mathrm{nat}}}{2}}{\hbar(\omega - \omega_0 + \frac{\Delta\omega_{\mathrm{Q}}}{2}) + i\frac{\Gamma_{\mathrm{nat}}}{2}} + \frac{\frac{\Gamma_{\mathrm{nat}}}{2}}{\hbar(\omega - \omega_0 - \frac{\Delta\omega_{\mathrm{Q}}}{2}) + i\frac{\Gamma_{\mathrm{nat}}}{2}}\right)\right] \tag{9}$$

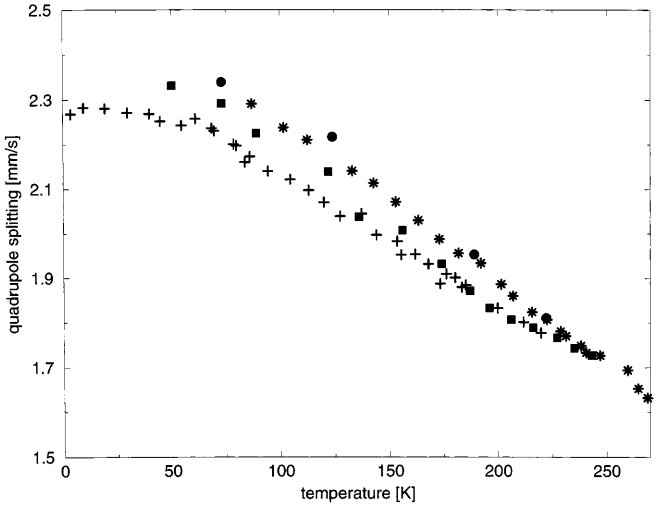

Fig. 3 The temperature dependence of the quadrupole splitting of deoxymyoglobin. *Filled squares*: data obtained from nuclear forward scattering using Eqs. (1), (2), (7) and (9) measured at the APS. *Filled circles*: data obtained from nuclear forward scattering using Eqs. (1), (2), (7) and (9) measured at the ESRF. *Stars and crosses*: data obtained from conventional Mössbauer absorption spectroscopy (stars: Parak et al. 1987; crosses: Eicher et al. 1974)

It is interesting to note that a shift of the absolute energy value of the resonances, leaving the quadrupole splitting unchanged, causes a phase shift of the forward scattered field amplitude $B_{\mathrm{tr}}(t)$, but does not change the forward scattered intensity. Therefore, ω_0 can be neglected.

The refractive index defined in Eq. (9) was used to evaluate the data. The FWHM of the broadening function was kept fixed $\Delta = 1.2\Gamma_{\mathrm{nat}}$. This Δ value has shown to be reasonable for proteins by conventional Mössbauer absorption spectroscopy (Parak et al. 1982). The parameters $\Delta\omega_{\mathrm{Q}}, T_{\mathrm{eff}}$ and E_0 were determined by least squares fits of the spectra using Eqs. (1), (2), (7) and (9). Some of the fitted spectra are shown in Figs. 1 and 2. The fits using a broadening function of Lorentzian type are in better agreement with the experimental data than the fits using a Gaussian broadening function. The temperature dependence of the quadrupole splitting $\hbar\Delta\omega_{\mathrm{Q}}$ of deoxymyoglobin obtained from these fits (assuming a Lorentzian broadening) is shown in Fig. 3. The quadrupole splittings assuming a Lorentzian or a Gaussian broadening agree within 0.02 mm/s. The $\langle x^2 \rangle$ values have been evaluated from the effective thickness T_{eff} assuming a linear temperature behaviour below 180 K and a broadening of Lorentzian shape. The results are shown in Fig. 4. The mean square displacements $\langle x^2 \rangle$ determined from the measurements at the APS increase dramatically at temperatures above 200 K, as known from conventional Mössbauer spec-

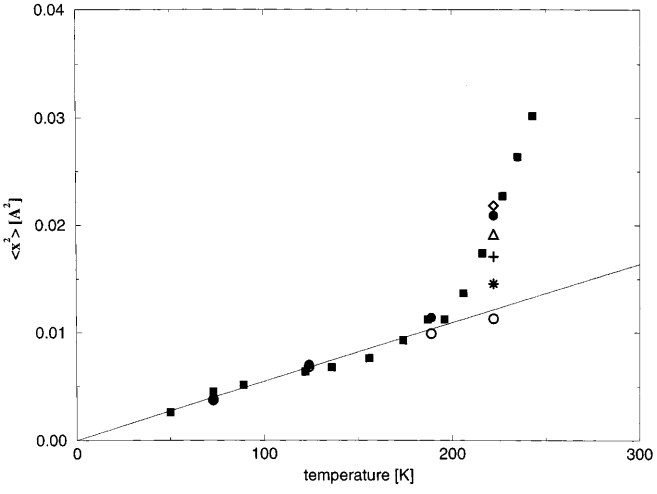

Fig. 4 Temperature dependence of the mean square displacement, $\langle x^2 \rangle$, of the iron in deoxymyoglobin. A distribution of Lorentzians with FWHM $\Delta = 1.2\Gamma_{\mathrm{nat}}$ is assumed for data evaluation. *Filled squares*: experiments performed at APS and evaluated between 25 ns and 118 ns using Eqs. (1), (2), (7) and (9). All other $\langle x^2 \rangle$ values are determined from the measurements performed at the ESRF. *Filled circles*: Eqs. (1), (2), (7) and (9) are used to evaluate the data between 25 ns and 118 ns. *Open circles*: Eqs. (1), (2), (7) and (9) are used to evaluate the data between 10 ns and 152 ns. All other least squares fits are obtained taking into account additional broad resonances using Eqs. (1), (2), (7) and (10). The data are evaluated between 10 ns and 152 ns. *Diamond*: $\Gamma_{\mathrm{b}} = 10\Gamma_{\mathrm{nat}}$ at 222 K. *Triangle*: $\Gamma_{\mathrm{b}} = 15\Gamma_{\mathrm{nat}}$ at 222 K. *Cross*: $\Gamma_{\mathrm{b}} = 20\Gamma_{\mathrm{nat}}$ at 222 K. *Star*: $\Gamma_{\mathrm{b}} = 25\Gamma_{\mathrm{nat}}$ at 222 K. *Solid line*: least squares fit to a first-order polynomial of the $\langle x^2 \rangle$ values taken at the APS at temperatures below 180 K. This way the $\langle x_{\mathrm{v}}^2 \rangle$ values are determined

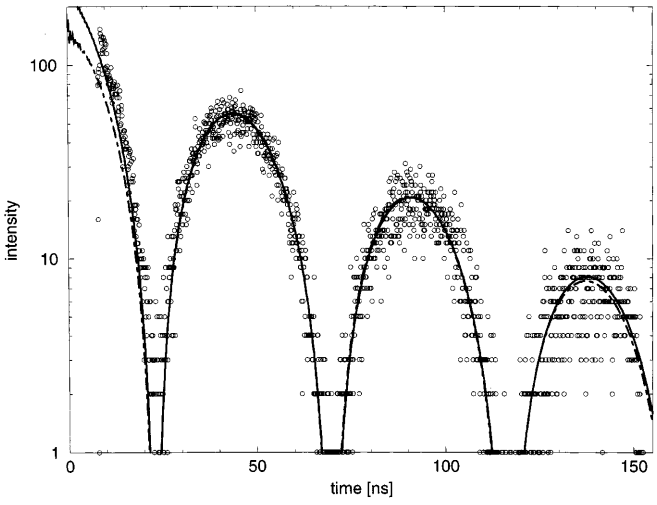

Fig. 5 Nuclear forward scattering spectrum of deoxymyoglobin taken at the ESRF at 222 K evaluated in the time range between 25 ns and 152 ns. *Dashed line*: least squares fit using Eqs. (1), (2), (7) and (9). *Solid line*: least squares fit with an additional broad line of $\Gamma_b = 15\Gamma_{nat}$ using Eqs. (1), (2), (7) and (10)

troscopy. However, the $\langle x^2 \rangle$ values measured at the ESRF seem to follow a linear temperature dependence up to 222 K.

In order to understand this different behaviour one has to compare the two experimental series. A broadening function of Lorentzian shape is assumed in the following. While at the APS the data collection starts at 25 ns, it starts at 10 ns at the ESRF. If the spectra taken at the ESRF and APS are evaluated in the same time range between 25 ns and 118 ns, the $\langle x^2 \rangle$ values of the two series agree (Fig. 4). At temperatures below 200 K these fits of the spectra measured at the ESRF are very satisfactory in the whole time window between 10 ns and 152 ns. However, the agreement between fit and experimental data taken at the ESRF at 222 K is very poor at times shorter than 20 ns (compare Fig. 5). As mentioned in the Introduction, broad Mössbauer lines would reveal themselves at short times. In order to check if additional broad lines have to be taken into account, we introduced one more resonance of width Γ_B at the position of each resonance resulting in a refractive index $n(\omega)$:

$$n(\omega) = F(\omega) \otimes \left[1 - \frac{T_{\text{eff}}}{4kd} \left\{ \frac{\frac{\Gamma_{\text{nat}}}{2}}{\hbar(\omega - \omega_0 + \frac{\Delta\omega_Q}{2}) + i\frac{\Gamma_{\text{nat}}}{2}} + \frac{\frac{\Gamma_{\text{nat}}}{2}}{\hbar(\omega - \omega_0 - \frac{\Delta\omega_Q}{2}) + i\frac{\Gamma_{\text{nat}}}{2}} + s\left(\frac{\frac{\Gamma_B}{2}}{\hbar(\omega - \omega_0 + \frac{\Delta\omega_Q}{2}) + i\frac{\Gamma_B}{2}} + \frac{\frac{\Gamma_B}{2}}{\hbar(\omega - \omega_0 - \frac{\Delta\omega_Q}{2}) + i\frac{\Gamma_B}{2}} \right) \right\} \right] \quad (10)$$

For the data evaluation a scaling factor

$$s = \exp\left[k^2(\langle x^2 \rangle - \langle x_v^2 \rangle)\right] - 1 \quad (11)$$

was used. $\langle x_v^2 \rangle$ is the part of the mean square displacement which is caused by vibrational motions. The $\langle x^2 \rangle$ and the $\langle x_v^2 \rangle$ values are taken from the data evaluation of the spectra from 25 ns on. While $\langle x^2 \rangle$ represents the total mean square displacements, the $\langle x_v^2 \rangle$ values have been determined by a linear regression of the $\langle x^2 \rangle$ values from $T = 50$ K to $T = 180$ K. The $\langle x_v^2 \rangle$ values at higher temperature were obtained by a linear extrapolation. Taking into account broad lines of widths in the range $10\Gamma_{nat} < \Gamma_b < 30\Gamma_{nat}$ for data evaluation, the least squares fit to the spectrum taken at the ESRF at 222 K is improved significantly. This is shown in Fig. 5. The fits using additional broad resonances of widths in the range $10\Gamma_{nat} < \Gamma_b < 30\Gamma_{nat}$ are of similar quality, but the obtained values for the effective thicknesses T_{eff} differ. The resulting $\langle x^2 \rangle$ values for different Γ_b values are shown in Fig. 4. Assuming $\Gamma_b = 15\Gamma_{nat}$ at 222 K, best agreement between the results of the measurements at the APS and ESRF is achieved. The mean square displacements agree very well with the $\langle x^2 \rangle$ values obtained with conventional Mössbauer spectroscopy (Parak et al. 1982). Applying the same procedure to the spectra measured at the APS, nothing is changed. Least squares fits taking into account additional resonances of widths in the range $10\Gamma_{nat} < \Gamma_b < 30\Gamma_{nat}$ are of same quality as the fits neglecting the broad resonances. Furthermore, the values obtained for the effective thicknesses and the quadrupole splittings agree.

Discussion

Our first result of this study is that nuclear forward scattering of synchrotron radiation yields the same result as conventional Mössbauer absorption spectroscopy but in a measuring time which is at least a factor of 10 shorter. This advantage helps us to obtain more accurate data and to investigate under conditions where conventional absorption spectroscopy may fail. Even in this first attempt to investigate the dynamic properties of a protein we improved our understanding of protein dynamics. In conventional Mössbauer absorption spectroscopy the measured Lamb-Mössbauer factors, and so the mean square displacement of the iron, is strongly influenced by the analogous parameter of the radioactive source. In addition, the dynamics in the laboratory frame is measured so that vibrations of the equipment itself must carefully be avoided. In contrast, in the present nuclear forward scattering investigation, solely the dynamics of the protein is measured. Also the measured time dependence of the forward scattering, according to the linewidth in the absorption experiment, is solely determined by the protein itself. Moreover, it is clearly shown that additional broad lines are necessary to interpret the nuclear forward scattering at short times and elevated temperatures. Using successfully the scaling

factor s of Eq. (11) for the contribution of the broad lines implies that they are caused by quasielastic scattering processes. The quasielastic scattering accounts completely for the difference of $\langle x^2 \rangle$ and $\langle x_v^2 \rangle$. Therefore, the present results support strongly the picture that protein dynamics below 200 K is dominated by harmonic processes which can be described by normal modes (Melchers et al. 1996). In the physiological relevant temperature regime, normal modes are insufficient to understand protein dynamics. Some degrees of freedom of the system are responsible for the diffusive motions in limited space which are protein specific and essential for the functional properties. For the future, a reduction of the detector system dead time is desirable in order to analyse the functionally important broad lines in more detail.

Inhomogeneous line broadening is normally taken into account by a Gaussian distribution of Lorentzians. It reflects the conformational substates (Frauenfelder et al. 1988), i.e. small structural differences of the individual molecules. In Mössbauer absorption spectroscopy on myoglobin we were not able to differentiate between a Gaussian distribution and a possible Lorentz distribution of Lorentzians. Astonishingly, the present experiments favour clearly a Lorentzian distribution of Lorentzians. While Gaussian distributions account for statistical differences in the environment, Lorentzian distributions are only known for distributed dipolar interactions (Stoneham 1969). A possible origin could be an interaction of the nuclear spin of the iron with the spins of the surrounding H nuclei. In this context we want to draw attention again to the exceptional advantage that the nuclear forward scattered intensity of synchrotron radiation is almost exclusively determined by the properties of the sample under investigation and not by parameters of the Mössbauer radiation source.

In both Mössbauer techniques the inhomogeneous broadening complicates the extraction of the parameters which characterise the dynamics. For the time dependence of the nuclear forward scattering intensity, $I(t)$, Smirnov (1996) showed that the following relationship is valid for Lorentzian broadened resonances and for relatively short times, e.g. small effective thicknesses:

$$I(t) \propto \exp\left[-\left(\frac{T_{\text{eff}}}{4} + \frac{\Delta}{\Gamma_{\text{nat}}} + 1\right)\frac{\Gamma_{\text{nat}} t}{\hbar}\right] \qquad (12)$$

The width Δ and the effective thickness T_{eff} influence the forward scattered intensity in a similar way. It was not possible to determine T_{eff} and Δ separately. In fits of the time spectra using a Lorentzian broadening function the width $\Delta = 1.2\Gamma_{\text{nat}}$ has been used. With proper experimental conditions this problem can be solved unambiguously. The nuclear forward scattering spectra of deoxymyoglobin show an oscillatory behaviour in time, which is caused by interference between the two resonances. This beat is referred as the "quantum beat" in the literature (Tramell and Hannon 1978). In general, time spectra are additionally modulated by so-called "dynamical beats", which are determined by the effective thickness T_{eff} (Kagan et al. 1979). In our experiments this beating is not observed because the accessible time window was too small. The first minimum of the "dynamical beats" is exclusively determined by the effective thickness T_{eff} (Smirnov 1996). At 50 K the effective thickness is $T_{\text{eff}} = 23$ for our measurements at the APS. The first minimum is situated at 180 ns and a time window up to 200 ns after the prompt pulse should be sufficient to determine Δ and T_{eff} independently in this case. If a larger time window for the measurements would be available, so that as a result this first minimum would occur inside this time window, the effective thickness could be determined from this minimum and therefore Δ and T_{eff} could be obtained independently.

Acknowledgements This work was supported by the BMBF Projektträger DESY-HS under the contracts 05SK8WOC and 05SK8WOA. The authors are grateful to W. Potzel for collaboration and fruitful discussions.

References

Achterhold K, Keppler C, Bürck U van, Potzel W, Schindelmann P, Knapp EW, Melchers B, Chumakov AI, Baron AQR, Rüffer R, Parak F (1996) Temperature dependent inelastic X-ray scattering of synchrotron radiation on myoglobin analysed by the Mössbauer effect. Eur Biophys J 25: 43–46

Alp EE, Mooney TM, Toellner T, Sturhahn W (1994) Nuclear resonant scattering beamline at the Advanced Photon Source. Hyperfine Interact 90: 323–334

Baron AQR (1995) Report on the X-ray efficiency and time response of a 1 cm^2 reach through avalanche diode. Nucl Instrum Methods A352: 665–667

Bürck U van, Siddons DP, Hastings JB, Bergmann U, Hollatz R (1992) Nuclear forward scattering of synchrotron radiation. Phys Rev B 46: 6207–6211

Debrunner PG (1993) Mössbauer spectroscopy of iron proteins. In: Berliner L, Reuben J (eds) Biological magnetic resonance, vol 13. Plenum Press, New York, pp 59–101

Eicher H, Parak F, Bade D, Tejada J (1974) Electronic structure of the iron in deoxygenated myoglobin from Mössbauer spectroscopy. J Phys C 6: 363–366

Frauenfelder H, Parak F, Young RD (1988) Conformational substates in proteins. Annu Rev Biophys Chem 17: 451–479

Hastings JB, Siddons DP, Bürck U van, Hollatz R, Bergmann U (1991) Mössbauer spectroscopy using synchrotron radiation. Phys Rev Lett 66: 770–773

Kagan Yu, Afanas'ev AM, Kohn VG (1979) On the excitation of isomeric nuclear states in a crystal by synchrotron radiation. J Phys C 12: 615–631

Keppler C, Achterhold K, Ostermann A, Bürck U van, Potzel W, Chumakov AI, Rüffer R, Parak F (1997) Determination of the phonon spectrum of iron in myoglobin using inelastic X-ray scattering of synchrotron radiation. Eur Biophys J 25: 221–224

Knapp EW, Fischer SF, Parak F (1983) The influence of protein dynamics on Mössbauer spectra. J Chem Phys 78: 4701–4711

Melchers B, Knapp EW, Parak F, Cordone L, Cupane A, Leone M (1996) Structural fluctuations of myoglobin from normal modes, Mössbauer-, Raman- and absorption-spectroscopy. Biophys J 70: 2092–2099

Parak F, Frauenfelder H (1993) Protein dynamics. Physica A 201: 332–345

Parak F, Reinisch L (1986) Mössbauer effect in the study of structure dynamics. In: Hirs L, Timosheff SN (eds) Methods

in enzymology, vol 131. Academic Press, New York, pp 568–607
Parak F, Knapp EW, Kucheida D (1982) Protein dynamics – Mössbauer spectroscopy on deoxymyoglobin crystals. J Mol Biol 161: 177–194
Parak F, Hartmann H, Nienhaus GU (1987) The Mössbauer effect as a probe of protein dynamics In: Austin R, Buhks E, Chance B, de Vault D, Gutton PL, Frauenfelder H, Gol'danskii VI (eds) Proceedings of life sciences. Springer, New York Berlin Heidelberg, pp 65–84
Rüffer R, Chumakov AI (1996) Nuclear resonance beamline at ESRF. Hyperfine Interact 97/98: 589–606
Shvyd'ko Yu, Bürck U van, Potzel W, Schindelmann P, Gerdau E, Leupold O, Metge J, Rüter HD, Smirnov GV (1998) Hybrid beat in nuclear forward scattering of synchrotron radiation. Phys Rev B 57: 3552–3561
Smirnov GV (1996) Nuclear resonant scattering of synchrotron radiation. Hyperfine Interact 97/98: 551–588
Stoneham AM (1969) Shapes of inhomogeneously broadened resonance lines in solids. Rev Mod Phys 41: 82–108
Teale FWJ (1959) Cleavage of the haem-protein link by acid methylethylketone. Biochim Biophys Acta 35: 543
Toellner TS, Hu M, Sturhahn W, Quast K, Alp EE (1997) Inelastic nuclear scattering with sub-meV energy resolution. Appl Phys Lett 71: 2112–2114
Tramell GT, Hannon JP (1978) Quantum beats from nuclei excited by synchrotron pulses. Phys Rev B 18: 165–172; erratum: Phys Rev B 19: 3835–3836